Chemically Tunable Nanoscale Propellers of Liquids

Boyang Wang and Petr Král*

Department of Chemistry, University of Illinois at Chicago, Chicago, Illinois 60607, USA

(Received 10 April 2007; published 28 June 2007)

We explore the limits of liquid pumping by "classical propellers" with molecular-scale blades. Our molecular dynamics simulations reveal a huge sensitivity of pumping to the chemistry of the blade-liquid interface. We demonstrate selective pumping of hydrophobic and hydrophilic liquids, where the pumping rate is determined by the effective profile of the solvated nanoscopic blades. These results have important implications for a potential design and assembly of molecular pumps and motile devices.

DOI: 10.1103/PhysRevLett.98.266102 PACS numbers: 81.07.Nb, 05.70.Np, 83.50.Ha

Recent studies have demonstrated efficient dragging of molecules at the nanoscale, based on their Coulombic scattering with asymmetrically moving electrons [1–3], ions, or polar molecules [4], in analogy to biological proton pumps [5]. Sensitive detection of molecular flows has also been proposed and tested [6–9]. We could also build nanoscale systems that might selectively transport and dynamically sieve fluids in numerous physical, chemical, and biological applications [10].

In this work, we show that this ambitious goal could be realized by nanoscopic propellers designed by robust macroscopic principles and possessing "chemically tunable" blades. In Fig. 1, we present the bulk (left) and surface (right) propellers in water solvent that are formed by functionalized carbon nanotubes (CNT) [11]. The bulk propeller can pump liquid along the tube z axis by two blades formed by pyrene molecules, attached to the opposite sides of the (8,0) CNT and tilted with respect to its axis, due to two chiral centers. The surface propeller pumps water orthogonal to the tube axis by four larger blades (see inset of Fig. 5) aligned straight along the axis. With the advances in synthetic chemistry, these systems could be realized by cyclic addition reactions [12].

Let us first examine the bulk propeller, shown in Fig. 1, with two different possible chemical designs. We focus on the hydrophobic or hydrophilic character of liquids, but other (chemical or biological) features can be considered as well. In the "hydrophobic" propeller, the charges of the H atoms at the tips of the pyrene blades are set to be $0.12e$, and those of the nearest aromatic carbon atoms to be $-0.12e$. In the "hydrophilic" propeller, these charges are chosen to be $0.30e$ and $-0.30e$, respectively. In this way, we model polar bonds present at the blade tips [13].

The propellers are embedded inside different solvents in the box of $2.5 \times 2.5 \times 4.4$ nm^3, with periodic boundary conditions applied. One dummy fixed atom is positioned outside each of the two CNT ends to fix their positions, and the tube is left free to vibrate. A torque $\mathcal{T}$ is applied to the two ends of the CNT rotor. In the molecular dynamics simulations with the NAMD package [14–17], we use the NPT ensemble, and choose a small Langevin damping, 0.01 ps^{-1}, in order to minimize the unphysical loss of momenta to the reservoirs [4].

In Fig. 2, we present the temperature dependence of the rotation (up) and pumping (down) rates of the bulk hydrophobic and hydrophilic propellers obtained in the hydrophobic dichloromethane (DCM) and hydrophilic water solvents. The results are obtained in averaging over a trajectory with ≈ 50 rotations for the applied torque of $\mathcal{T} = 0.2$ nN nm. As the systems are heated above the (normal) freezing points of the solvents, $T_f^{\mathrm{DCM}} = 175$ K and $T_f^{\mathrm{water}} = 273$ K, the rotation rates grow, due to smaller solvent viscosities. The hydrophilic propeller rotates slower, since its polar blades interact stronger with both solvents. Substantially slower rotation occurs in water that forms hydrogen bonds with its polar blades [18] [see inset in Fig. 2 (down)].

The results agree with the Stokes' law that is largely valid at the nanoscale even in the presence of slipping boundary conditions [19,20]. We can write it as $\mathcal{T} \approx K\mu\omega$, where K is a constant determined by the shape of the propeller, μ is the dynamic viscosity, and ω is the angular velocity of the rotation. Since the viscosity is

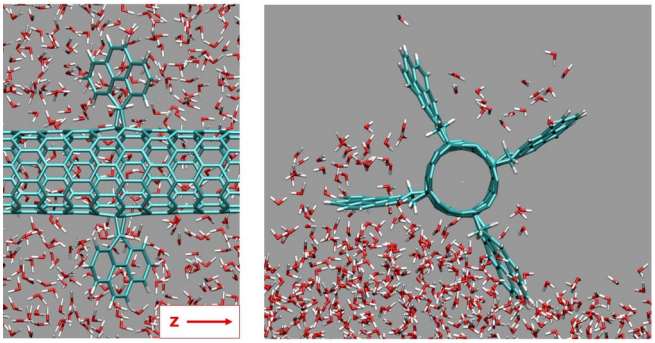


FIG. 1 (color online). The bulk (left) and surface (right) water propellers that pump water along the tube (z) axis and orthogonal to it, respectively. Both systems are based on the (8,0) CNTs and have covalently attached aromatic (hydrophobic) blades. Water is partly removed from the front to uncover detail of the propellers.

 © 2007 The American Physical Society

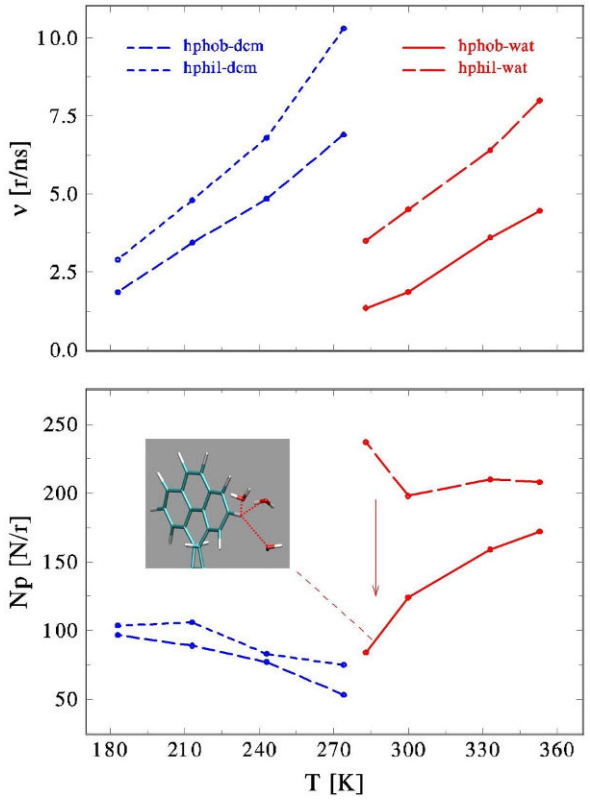


FIG. 2 (color online). (up) The rotation rates (round/ns) of the bulk hydrophobic (''pho'') and hydrophilic (''phi'') propellers in water and DCM solvents as a function of temperature. (down) The pumping rates (molecules/round) of these propellers. (inset) Formation of hydrogen bonds between the hydrophilic blades and water can dramatically reduce the pumping rate.

$\mu \propto 1/T$ [21], the angular velocity $\omega = 2\pi\nu$ is approximately proportional to temperature for a constant torque $\mathcal{T}$, in agreement with Fig. 2 (up). The angular-momentum dissipation rate, which limits the steady-state rotation of the propeller in the presence of weak driving, could be obtained from the equilibrium fluctuations of its rotation angle [22].

Solvent molecules are pumped by direct and indirect (mediated by other molecules) collisions with the propeller's blades. If they were noninteracting point particles (ideal gas), one would expect that all the molecules present in the volume that the blades can reach at should be pumped out in a half rotation (two blades). This volume roughly fills the space between a cylinder of the radius $R_T \approx 0.45$ nm [the van der Waals (vdW) interaction radius of the CNT], and $R_B \approx 1.20$ nm (the same including the blades), and its length is $l_B \approx 1.1$ nm. The volume of this cylinder is decreased by the blades of the vdW thickness ≈ 0.35 nm. From the density of the solvent molecules, we can estimate that this ideal pumping rate is $P_m \approx 92$ DCM and 170 water molecules per round, which correlates well with the rates in Fig. 2. These rates are obtained from the average number of molecules that cross unidirectionally the box ends. To some extent, they are influenced by the presence of periodically arranged propellers (see discussion at Fig. 3).

The effective cross section and pumping rates of the molecular-scale blades can be dramatically changed by their interactions with the solvent molecules. In the DCM solvent, Coulombic and vdW interactions between the molecules and between them and the blades are weak, so the solvent molecules resemble ideal gas that ''slips'' on the blades in independent scattering events [23]. The same is true for the hydrophilic rotor, although weak Coulombic coupling of the blades and DCM slightly slows down the pumping. At high temperatures, momentum is dissipated faster and the pumping rate is reduced, as seen in Fig. 2 (down).

In the polar water solvent, molecules form clusters, transiently held together by hydrogen bonds [18]. This can effectively increase the cross section of the hydrophobic blades and the pumping rate over that estimated above by purely geometrical means, in agreement with Fig. 2. In the case of hydrophilic propeller, water forms relatively stable hydration shells around the blades [24] [inset in Fig. 2 (down)] that reduce the effective space available for a direct contact of the pumped molecules with the blades. Tilting of the ''dressed'' blades becomes also less recognizable by more distant water layers in classical Navier-Stokes flowing. This causes drastic reduction of the pumping rates with respect to the hydrophobic propeller, as shown by the vertical arrow in Fig. 2 (down). At high temperatures, the hydrogen bonds break down and the pumping rates increase and tend to be the same in both types of propellers.

Figure 3 illustrates the axial and radial distributions of the average longitudinal velocity, v_z (along the tube axis), and the angular velocity, $v_\varphi = v_x \sin(\varphi) - v_y \cos(\varphi)$ (around the tube circumference), of water pumped at

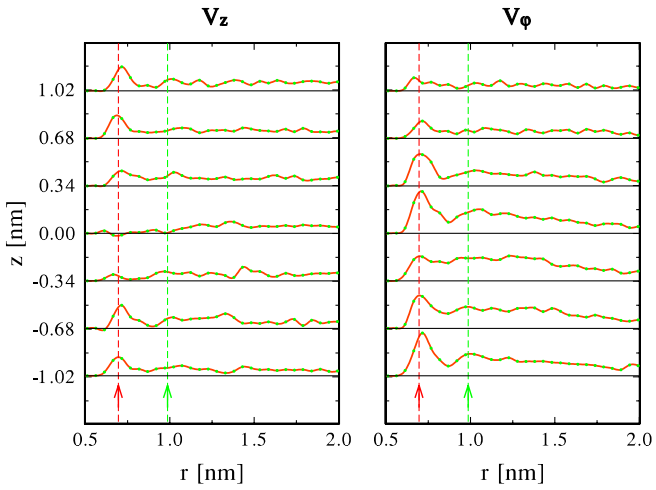


FIG. 3 (color online). The axial and radial distributions of the average longitudinal v_z (left) and angular v_φ velocities (right) of water molecules pumped by the hydrophobic propeller at $T = 300$ K. The approximate positions of the first and second water layers are clearly seen (arrows) [25].

$T = 300$ K by the hydrophobic propeller. Here, φ is the angular coordinate of the oxygen atoms in the plane perpendicular to the tube axis. Pumping is realized by the torque of $\mathcal{T} = 0.2$ nN nm from negative to positive z in the cell of $4.6 \times 4.6 \times 4.6$ nm^3, with 13 longitudinal and 50 radial fictive boxes. Averaging is done over a large data set of 10^5 frames, separated by $\tau = 50$ fs intervals, where neighboring frames define the molecular shifts Δi ($i = x$, y, z) in time τ. We sum the velocities $v_i = \Delta i/\tau$ of all the oxygen atoms located in the same box in all the frames, divide this sum by the box volume, and plot the relative values. This sum is proportional to the average density of mass flow, i.e., the product of velocity and water density (assumed to be roughly constant).

The first two peaks, seen at small r in both v_z and v_φ, are located at the radial separations from the tube center of the first and second water layers, $r = 0.7$ and 1 nm, respectively [25]. These peaks signal relatively regular motion (mutual slipping) of the water layers already 0.3–0.5 nm away from the blade region. The molecular layers have also been observed in other simulations [26] and model studies [27] of flowing liquids. Around the blades ($z = 0$), the longitudinal molecular motion is highly irregular, $v_z \approx 0$, and the molecular momentum is not conserved, due to scattering with the blades. After integrating this v_z over the radial and angular coordinates, we found that the total water flows at different z differ by $<15\%$, due to approximations. At $z = 0$, v_φ has a large peak, induced by the rotating blades, while beyond the blades this swirling rapidly decays. Note also that the pumping rate for the system in Fig. 3 is about twice larger than that in Fig. 2, realized in ≈ 3.5 times smaller box. Therefore, the parallel propellers are here not influencing much each other.

The pumping rate should also depend on the relative size and shape of the molecules and the blades. We test the size dependence in pumping of n-alkanes, n-C_nH_{2n+2} ($n = 5 - 17$), which are in a liquid phase at $T = 300$ K and $P = 1$ atm [28]. These alkanes, especially the longer ones, are of the same size or larger than the blades of the approximate size 0.8×1.1 nm, as seen in Fig. 4. The number of molecules of each alkane is chosen such that they include roughly the same amount (5900) of atoms in the periodic box of $4.4 \times 4.4 \times 4.4$ nm^3.

In Fig. 4, we present how the alkanes are pumped with the hydrophobic propeller and the applied torque of $\mathcal{T} = 0.2$ nN nm. The smallest pumping rates are comparable to those obtained for water (1550 atoms/round) in the same box. The pumping rate increases until n-C_8H_{18}, since the blades can "grab" more atoms in larger molecules. In even longer alkanes, the number of atoms grabbed by the blades remains similar, but the number of atoms that are "left out" and hooked in between the other molecules grows. Releasing of these alkanes by the moving blades is hampered by significant alkane-alkane interactions, causing the drop of pumping rates.

It is also interesting to realize pumping of molecules on the surfaces of liquids, often covered by molecular monolayers of other materials. We investigate briefly pumping of water with the surface propeller shown in Fig. 1 (right). The blades in the hydrophilic and hydrophobic surface propellers have the same atomic charges as in the bulk case. The propellers are positioned parallel to the water surface, and the blades are partly immersed in it. We use 9×9 dummy atoms to support 3500 water molecules, placed in a periodic box of $5.5 \times 5.0 \times 9.0$ nm^3. The torque of $\mathcal{T} = 0.16$ nN nm that is applied to the system, described by the NVT ensemble [14].

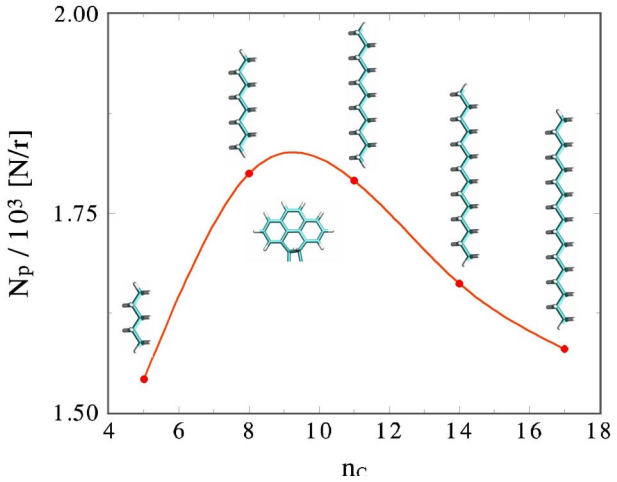


FIG. 4 (color online). Dependence of the pumping rate N_P on the number n_C of carbons in the lipid molecule n-C_nH_{2n+2} ($n = 5 - 17$), used in the pumped solvent. The lipids are comparable in size to the blade, shown in the inset.

In Fig. 5, pumping of water by the surface propellers is shown as a function of the height of their mounting. During pumping, the propellers need to push their blades through the water surface. This can be resisted by surface tension, depending on the blade's chemical and structural parameters, the height of the rotor's mounting, and its angular velocity. Once the blades penetrate the water, the molecules are adsorbed to them and the rotor's body, and they can remain there during the rotation. In the inset of Fig. 5, we can see their accumulation in the back of the hydrophobic propeller; for clarity, water is partly removed from the front of the submerged blade.

The presence of surface tension and molecular adhesion in this dynamical heterogeneous system requires to apply a certain minimal torque to rotate the propeller. At high temperatures, the propeller can only pump molecules that are lifted up by thermal expansion and excitation. The last option is relevant for the hydrophobic propeller only at $T = 350$ K, where pumping at heights above $h = 0.3$–0.4 nm is possible with rates $N_P < 500$. Here, the propeller can rotate fast and irregularly, so it might chop water molecules off the surface and carry them around, as shown in Fig. 1 (right). At lower temperatures, pumping is possible only at lower heights. The pumping rate increases more or less linearly with the depth of the blades, and when the rotor submerges together with the blades, additional

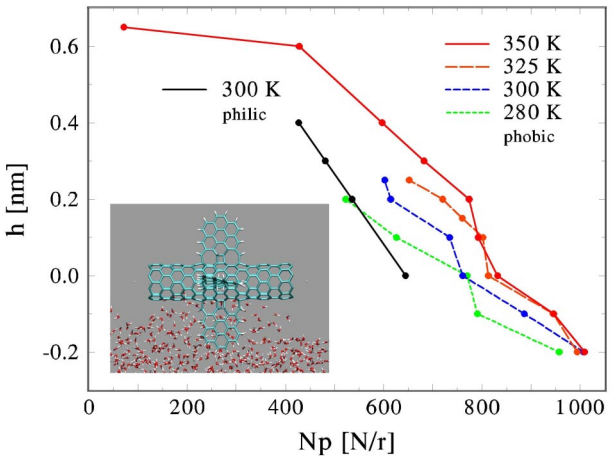


FIG. 5 (color online). Dependence of the pumping rate N_P of water by the hydrophobic and hydrophilic propellers on the height of their mounting. (inset) Water around the hydrophobic propeller, mounted at the height of $h = 0.1$ nm and pumping in the back, orthogonal to the tube axis.

breaks emerge in it. The pumping rates of the hydrophilic propeller at $T = 300$ K are smaller, as in the bulk propeller, and depend less on the height, due to the attraction of water to the blades (see attached movies [29]).

We have introduced nanoscale propellers of liquids and demonstrated that their pumping efficiency is highly sensitive to the size, shape, chemical, or biological compositions of their ''coral-like'' blades. In practical applications, the propellers could be mounted into CNT bearings [30] and rotated by mechanical, optical [31–33], electrical [34], or chemical means [35], in analogy to molecular motors. These nanosystems could also work in reverse ''windmill'' modes [36,37] and could be used in artificial motile machines [38–40].

This work was partly done with the use of the computers at the National Computational Science Alliance.

*pkral@uic.edu

[1] P. Král and D. Tománek, Phys. Rev. Lett. **82**, 5373 (1999).
[2] B. C. Regan, S. Aloni, R. O. Ritchie, U. Dahmen, and A. Zettl, Nature (London) **428**, 924 (2004).
[3] K. Svensson, H. Olin, and E. Olsson, Phys. Rev. Lett. **93**, 145901 (2004).
[4] B. Wang and P. Král, J. Am. Chem. Soc. **128**, 15 984 (2006).
[5] P. D. Boyer, Annu. Rev. Biochem. **66**, 717 (1997).
[6] P. Král and M. Shapiro, Phys. Rev. Lett. **86**, 131 (2001).
[7] S. Ghosh, A. K. Sood, and N. Kumar, Science **299**, 1042 (2003); U.S. Patent No. 6 718 834 B1.
[8] A. K. Sood and S. Ghosh, Phys. Rev. Lett. **93**, 086601 (2004).
[9] C. Subramaniam, T. Pradeep, and J. Chakrabarti, Phys. Rev. Lett. **95**, 164501 (2005).
[10] K. Deguchi, S. Ito, S. Yoshioka, I. Ogata, and A. Takeda, Anal. Chem. **76**, 1524 (2004).
[11] J. Han, A. Globus, R. Jaffe, and G. Deardorff, Nanotechnology **8**, 95 (1997).
[12] D. Tasis, N. Tagmatarchis, A. Bianco, M. Prato, and Chem. Rev. **106**, 1105 (2006).
[13] F. Zhu and K. Schulten, Biophys. J. **85**, 236 (2003).
[14] J. C. Phillips *et al.*, J. Comput. Chem. **26**, 1781 (2005).
[15] M. Karplus *et al.*, J. Phys. Chem. B **102**, 3586 (1998).
[16] S. E. Feller, Y. H. Zhang, R. W. Pastor, and B. R. Brooks, J. Chem. Phys. **103**, 4613 (1995).
[17] T. Darden, D. York, and L. Pedersen, J. Chem. Phys. **98**, 10 089 (1993).
[18] K. A. T. Silverstein, A. D. J. Haymet, and K. A. Dill, J. Am. Chem. Soc. **122**, 8037 (2000).
[19] M. Vergeles, P. Keblinski, J. Koplik, and J. R. Banavar, Phys. Rev. E **53**, 4852 (1996).
[20] T. M. Squires and S. R. Quake, Rev. Mod. Phys. **77**, 977 (2005).
[21] A. V. Brancker, Nature (London) **166**, 905 (1950).
[22] J. Servantie and P. Gaspard, Phys. Rev. Lett. **97**, 186106 (2006).
[23] C. H. Choi, K. J. A. Westin, and K. S. Breuer, Phys. Fluids **15**, 2897 (2003).
[24] T. M. Raschke and M. Levitt, Proc. Natl. Acad. Sci. U.S.A. **102**, 6777 (2005).
[25] F. Moulin, M. Devel, and S. Picaud, Phys. Rev. B **71**, 165401 (2005).
[26] J. Gao, W. D. Luedtke, and U. Landman, Science **270**, 605 (1995).
[27] K. P. Travis, B. D. Todd, and D. J. Evans, Phys. Rev. E **55**, 4288 (1997).
[28] D. S. Viswanath and G. Natarajan, *Data Book on the Viscosity of Liquids* (Hemisphere Publishing Corporation, New York, NY, 1989).
[29] See EPAPS Document No. E-PRLTAO-98-061726 for movies of the water propeller pumping rates. For more information on EPAPS, see http://www.aip.org/pubservs/epaps.html.
[30] J. Cumings and A. Zettl, Science **289**, 602 (2000).
[31] P. Král and H. R. Sadeghpour, Phys. Rev. B **65**, 161401(R) (2002).
[32] J. Plewa, E. Tanner, D. M. Mueth, and D. G. Grier, Opt. Express **12**, 1978 (2004).
[33] S. Tan, H. A. Lopez, C. W. Cai, and Y. Zhang, Nano Lett. **4**, 1415 (2004).
[34] P. Král and T. Seideman, J. Chem. Phys. **123**, 184702 (2005).
[35] T. R. Kelly, H. De Silva, and R. A. Silva, Nature (London) **401**, 150 (1999).
[36] J. Vacek and J. Michl, Proc. Natl. Acad. Sci. U.S.A. **98**, 5481 (2001).
[37] G. S. Kottas, L. I. Clarke, D. Horinek, and J. Michl, Chem. Rev. **105**, 1281 (2005).
[38] R. Dreyfus *et al.*, Nature (London) **437**, 862 (2005).
[39] Y. Shirai *et al.*, J. Am. Chem. Soc. **128**, 4854 (2006).
[40] M. Manghi, X. Schlagberger, and R. R. Netz, Phys. Rev. Lett. **96**, 068101 (2006).